Electronic Supplementary Material (ESI) for Analyst.

Supporting Information – Multi-element stable isotope Raman microspectroscopy of bacterial carotenoids unravels rare signal shift patterns and single-cell phenotypic heterogeneity

Julian Weng, Kara Müller, Oleksii Morgaienko, Martin Elsner, and Natalia P. Ivleva*

Technical University of Munich, Institute of Water Chemistry, Chair for Analytical Chemistry, Lichtenbergstr. 4, 85748 Garching, Germany

E-mail: natalia.ivleva@tum.de

Phone: +49 (0) 89 289 54 507

Experimental - Supporting Information

Optimized M9 minimal medium composition with D-glucose as the sole carbon source

SI Table 1: Exact M9 minimal medium composition with D-glucose as the sole carbon source; optimized according to *Weiß et al.*[1]

Constituent		Molar mass [g/mol]	Concentration [mmol/L]
$Na_2HPO_4 \cdot 2\,H_2O$	M9 salt solution, pH 7	177.0	48
KH_2PO_4		136.1	22
NaCl		58.44	9.2
NH_4Cl		53.49	19
$MgSO_4 \cdot 7\,H_2O$		246.5	1.0
$CaCl_2 \cdot 2\,H_2O$		147.0	0.30
$FeSO_4 \cdot 7\,H_2O$		278.0	1.0×10^{-4}
$Co(NO_3)_2 \cdot 6\,H_2O$	Trace Metal Mix A5	291.0	1.7×10^{-4}
H_3BO_3		61.83	4.6×10^{-2}
$MnCl_2 \cdot 4\,H_2O$		197.9	9.1×10^{-3}
$ZnSO_4 \cdot 7\,H_2O$		287.5	7.7×10^{-4}
$Na_2MoO_4 \cdot 2\,H_2O$		242.0	1.6×10^{-3}
$CuSO_4 \cdot 5\,H_2O$		249.7	3.2×10^{-4}
D-glucose ($^{12}C_6/^{13}C_6$), $4\,g\,L^{-1}$		180.2/186.2	22

Recording of bacterial growth curves with a microplate reader

Monitoring of microbial growth under different medium compositions was performed with a multi-mode microplate reader (Synergy HT, BioTec Instruments Inc., Winooski, VT, USA). For each tested medium, triplicates of medium blank and medium inoculated with bacteria were prepared in 96-well-microplates (transparent, PS, Greiner Bio-One GmbH, Frickenhausen, Germany). Each well was filled with 200 µL of the respective sample and the microplates were sealed with transparent adhesive sheets (polyester, 50 µm thickness, SealPlate, Carl Roth GmbH, Karlsruhe, Germany). After inserting into the microplate reader,

plates were incubated at 37 °C with constant shaking. Optical density (OD) measurements at 600 nm were performed automatically by the device for each well at an interval of 30 min.

Determination of random measurement coordinates on the sample spot

For the measurement of SCRM spectra, a defined number of single cells were randomly chosen. For this, the sample spot on the Al-coated glass slide was approximated to be circular. The center and radian of the spot were determined with a 5× objective (Zeiss EC Epiplan-Neofluar HD, NA = 0.13, Zeiss, Oberkochen, Germany). With this, an in-house R script (R-4.0.3, R Core Team, Vienna, Austria) was used to calculate a set of random coordinates within the circular geometry. The motorized microscope stage was sequentially moved to the randomly generated x- and y-coordinates and the optical focus was laid manually on the nearest single bacterium cell.

Processing of raw single-cell Raman spectra

The processing of raw spectra with the in-house R script (R-4.0.3, R Core Team, Vienna, Austria) was done according to the following automated scheme:

First, the random shift in the wavenumber axis of each spectrum is corrected by referencing to the first order signal of a Si-wafer. A spectrum of this Si-wafer was acquired at the start of each measurement day. The exact position of the first order signal is determined by fitting a Gaussian density function to the respective band and extracting its mean. Subsequently, the shift is calculated and corrected by comparison to a fixed reference value. Spectra are cropped to a defined range and background-corrected using a *rolling ball* algorithm from the *baseline* package.[2] After that, spectra are min-max scaled using a function from the *caret* package[3] and mean spectra are calculated if desired. To determine approximate peak positions, a simple peak picking mechanism based on local maxima was implemented using a

function of the *IDPmisc* package.[4] For principal component analysis (PCA), a function of the *FactoMineR* package[5] was applied (same spectral range as for average spectra). Data visualization was carried out with the *ggplot2* package.[6] Furthermore, the packages *tibble* and *data.table* were utilized for data organization.[7,8]

For the individual spectra in Figure 1, a Savitsky-Golay filter was applied using a function of the *signal* package.[9] 3D visualization of the individual spectra in Figure 1 was carried out with the *rgl* package.[10]

Signal positions and FWHM from Gaussian fits

In order to determine exact signal positions, single-cell Resonance Raman (SCRR) signals were fitted with a Gaussian density function. First, preprocessed (background corrected and scaled) individual spectra were cropped to a range that fully comprised the investigated signal. The four parameters of a Gaussian density function g of the form $a + |b| * g(x, \mu, \sigma)$ (with the y-offset a, a positive scaling factor b, the Gaussian mean μ and the standard deviation σ) were fitted with a least squares algorithm. The means μ of the fitted Gaussian curves were extracted as the SCRR signal positions.

For the computation of the full width at half maximum (FWHM) of individual SCRR signals, the half maximum intensity at the Gaussian means μ (i.e. signal positions) were calculated. For the two halves of the signal peak, the wavenumbers corresponding to the half maximum intensity were extracted and the FWHM was obtained from their difference.

Signal integral ratios from Gaussian fits

Signal integral ratios of Resonance Raman and regular CH/CD-stretch signals were analyzed by fitting Gaussian density functions on the respective signals, similar as described above. However, the fit included the sum of two Gaussian functions with fixed mean (μ) parameter (i.e. defined wavelength of the signal position): $a + |b_1| * g(x, \sigma_1) + |b_2| * g(x, \sigma_2)$. Both Gaussian fit curves were integrated and the ratio $\mathrm{I_{signal\ A}}/(\mathrm{I_{signal\ A}} + \mathrm{I_{signal\ B}})$ was calculated.

Figures - Supporting Information

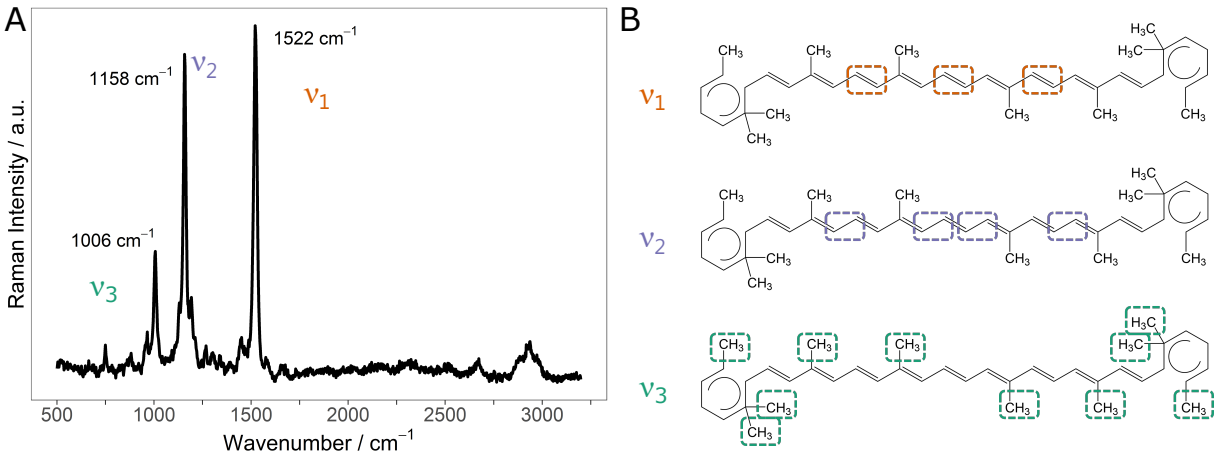

SI Figure 1: (A) Average single-cell Raman spectrum (n = 35) of *Sphingomonas sp.* acquired with an integration time of 2 s and a laser power of 1 mW (532 nm laser); the most prominent bands are designated as ν_1, ν_2 and ν_3; (B) general carotenoid structure with terminal rings. Structural elements that contribute to the most relevant Raman-active vibrations – C-double- and single-bond stretchings and methyl rocking vibrations – are marked and assigned to ν_1, ν_2 and ν_3.[11]

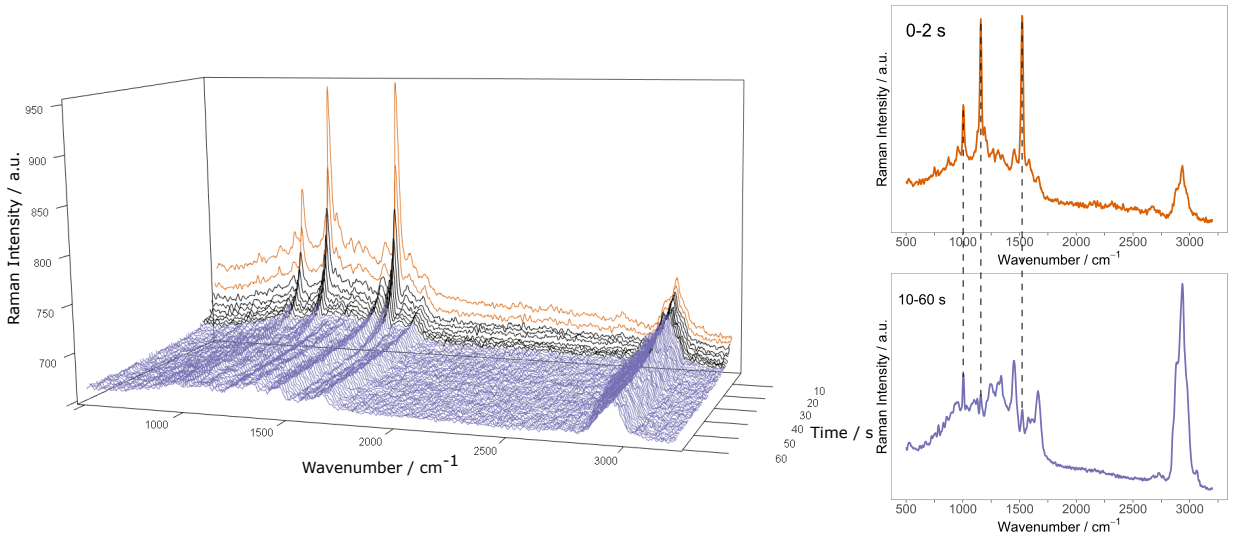

SI Figure 2: Time series of Raman spectra acquired from a single *Sphingomonas sp.* cell with integration intervals of 1 s (laser power: 3 mW); spectra were not background corrected or normalized but processed with a Savitsky-Golay filter (order 3 and window size 9); the plots to the right show integrations of the individual Raman spectra over the periods of 0 s to 2 s (orange) and 10 s to 60 s (blue).

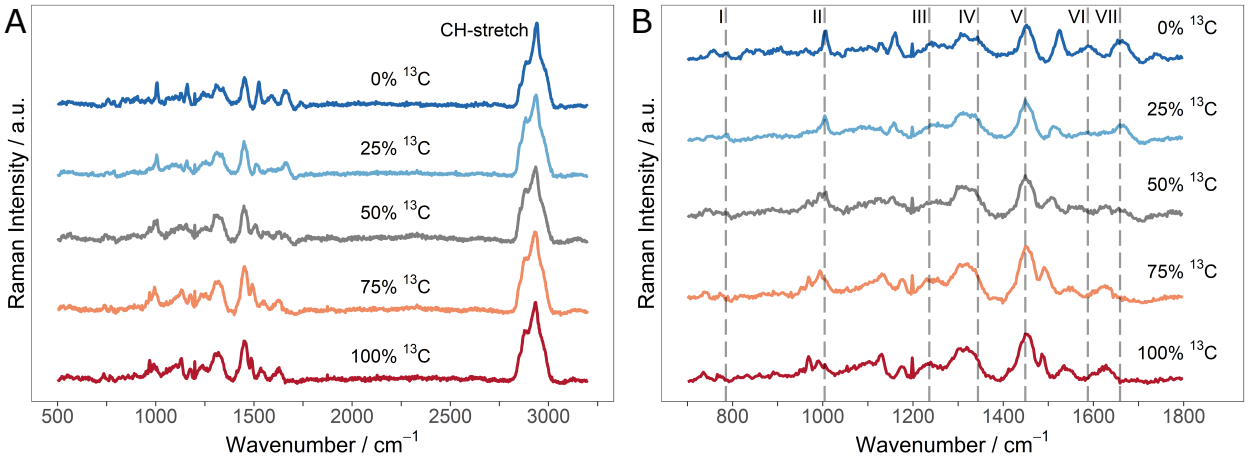

SI Figure 3: (A) Average single-cell Raman spectra (n = 30-40; 20 s integration time, 10 mW laser power) of *Sphingomonas sp.* grown in medium containing diverging ratios of $^{12}C_6$- and $^{13}C_6$-glucose; (B) fingerprint area zoom of the spectra (700 cm^{-1} to 1800 cm^{-1}) with selected signals assigned to cellular biomolecules as follows:[12,13] I – $\nu(C,U,T)_{ring}$, II – $(Phe)_{ring\ breathing}$, III – $\nu(Amide\ III)$, IV – $\delta(CH_2)_{rocking}$, V – $\delta(CH_2)_{scissor}$, VI – $\nu(G,A)_{ring}$, VII – $\nu(Amide\ I)$ where U, C, T, G, A and Phe stand for uracil, cytosine, thymine, guanine, adenine and phenylalanine (ν = stretching mode, δ = bending mode).

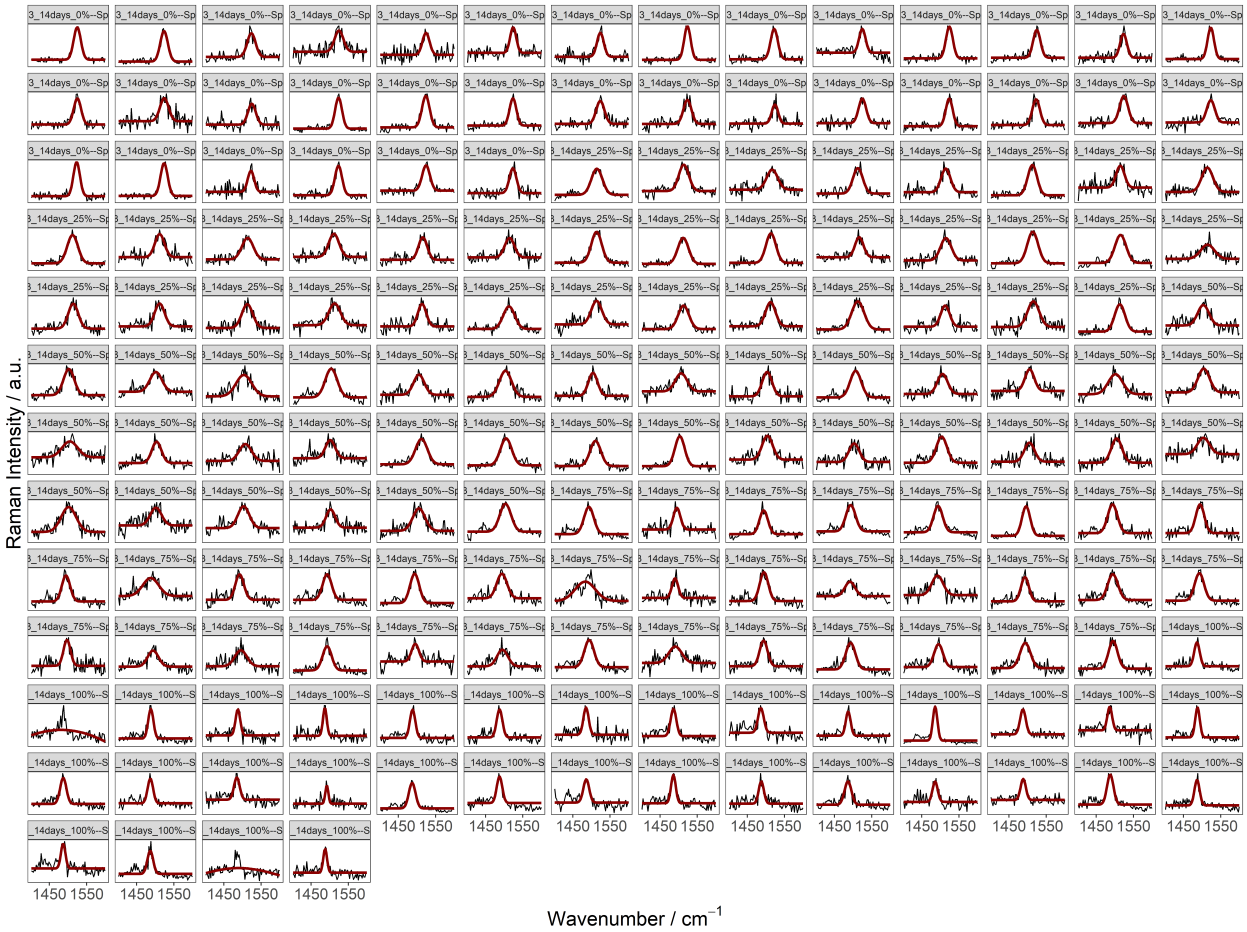

SI Figure 4: Facet plot of the ν_1-signal of individual spectra corresponding to the average single-cell Resonance Raman spectra of *Sphingomonas sp.* depicted in Figure 2 A; cells were grown in medium containing different ratios of $^{12}C_6$- and $^{13}C_6$-glucose, n = 35 per condition; overlayed red lines indicate the gaussian fits carried out for each spectrum.

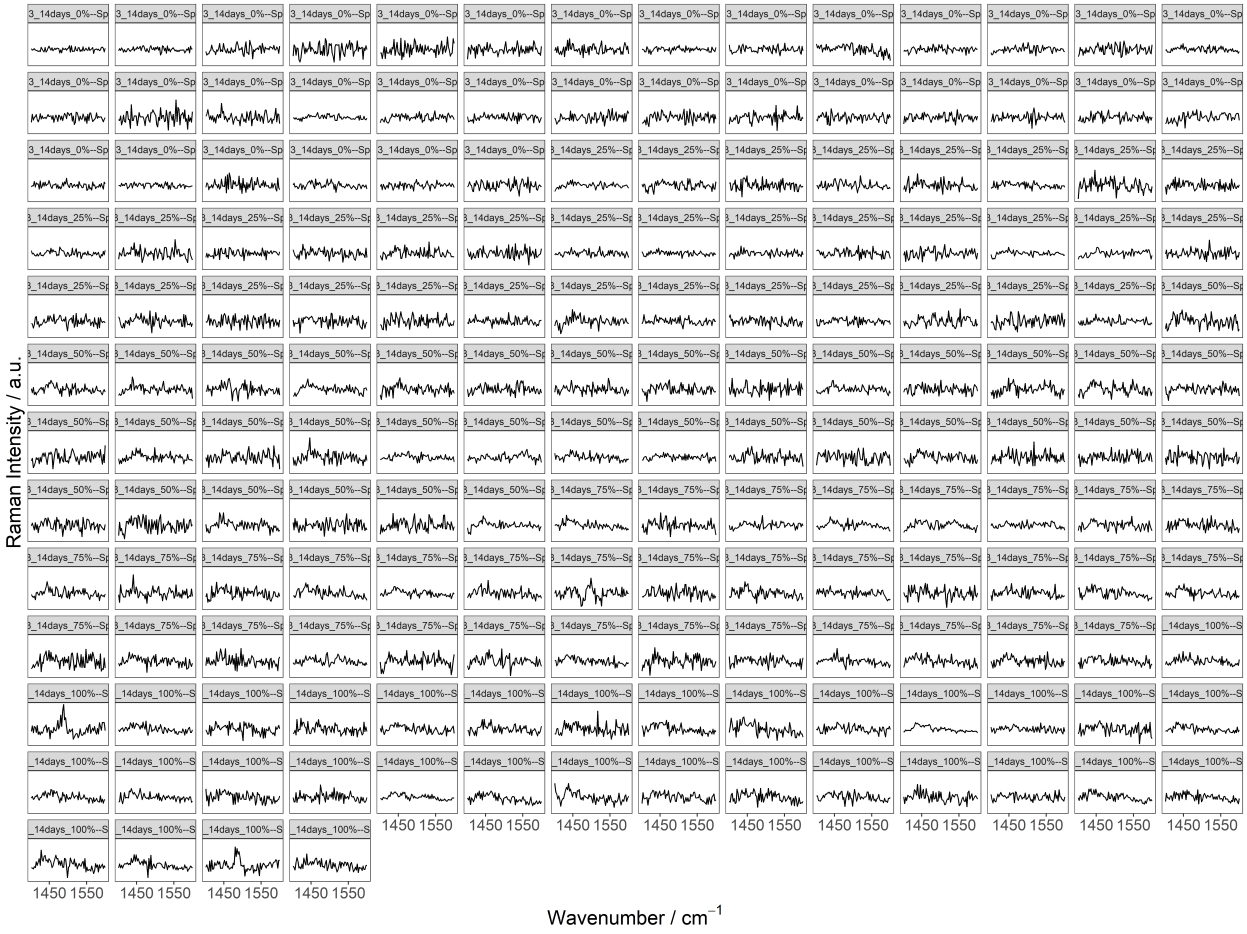

SI Figure 5: Residual spectra facet plot of the ν_1-signal of individual spectra and gaussian fits shown in SI Figure 4.

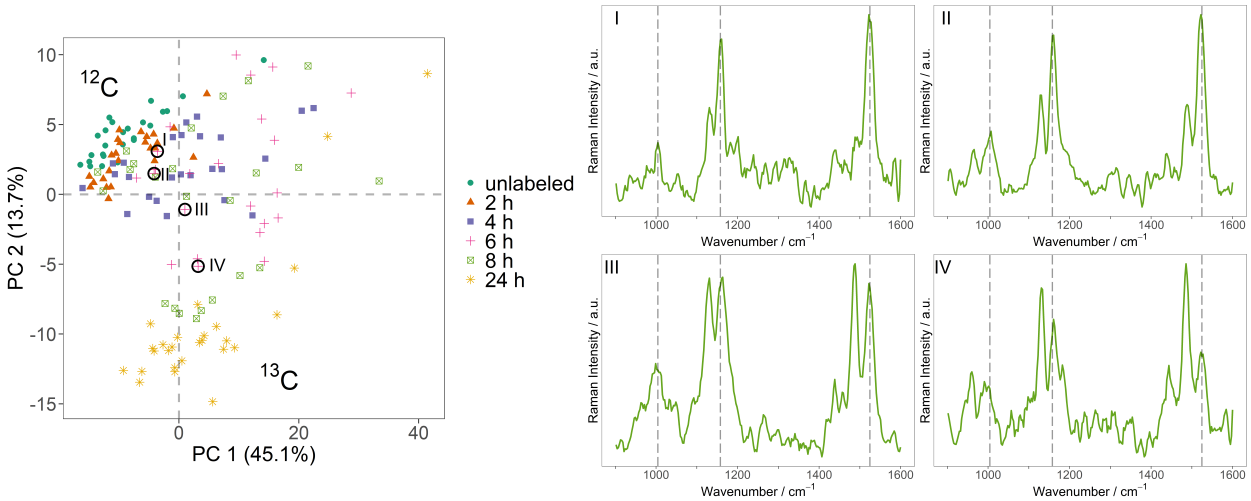

SI Figure 6: PCA scores plot (first and second PCA dimension) of the individual Resonance Raman spectra (n = 25) of unlabeled *Sphingomonas sp.* inoculated into $^{13}C_6$-glucose (as shown in Figure 3); spectra were acquired of unlabeled cells and cells harvested 2 h, 4 h, 6 h, 8 h and 24 h after the inoculation; in the scores plot, selected individual points of the 6 h sample were marked and the corresponding individual spectra are shown (processed with a Savitsky-Golay filter with order 3 and window size 9, dashed lines in the spectra correspond to the position of carotenoid signals of unlabeled bacteria).

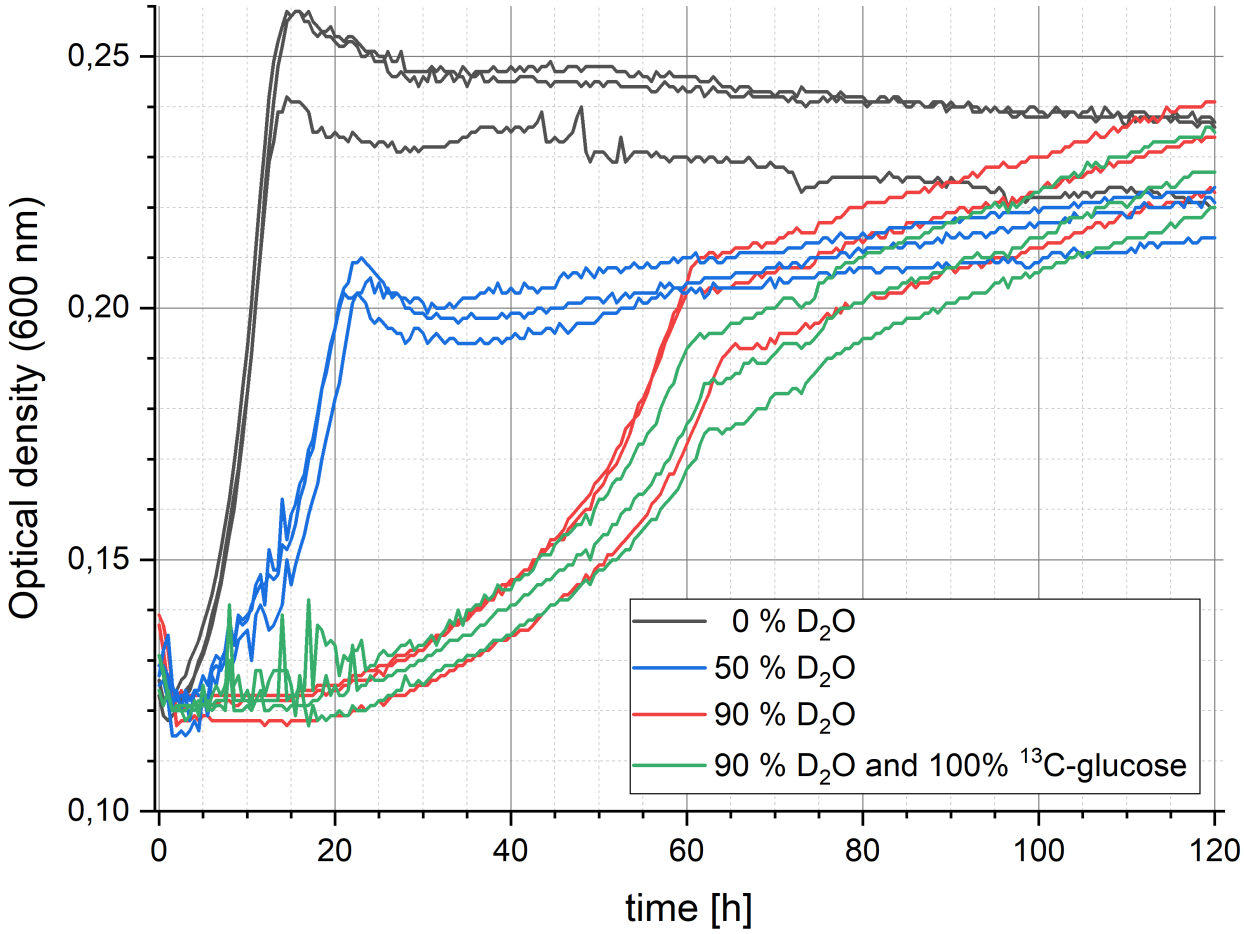

SI Figure 7: Growth curves of *Sphingomonas sp.* incubated with different ratios of H_2O/D_2O and either $^{12}C_6$-glucose or $^{13}C_6$-glucose (triplicates for each composition). Optical density at 600 nm was automatically recorded with a multi-mode microplate reader in time intervals of 30 min.

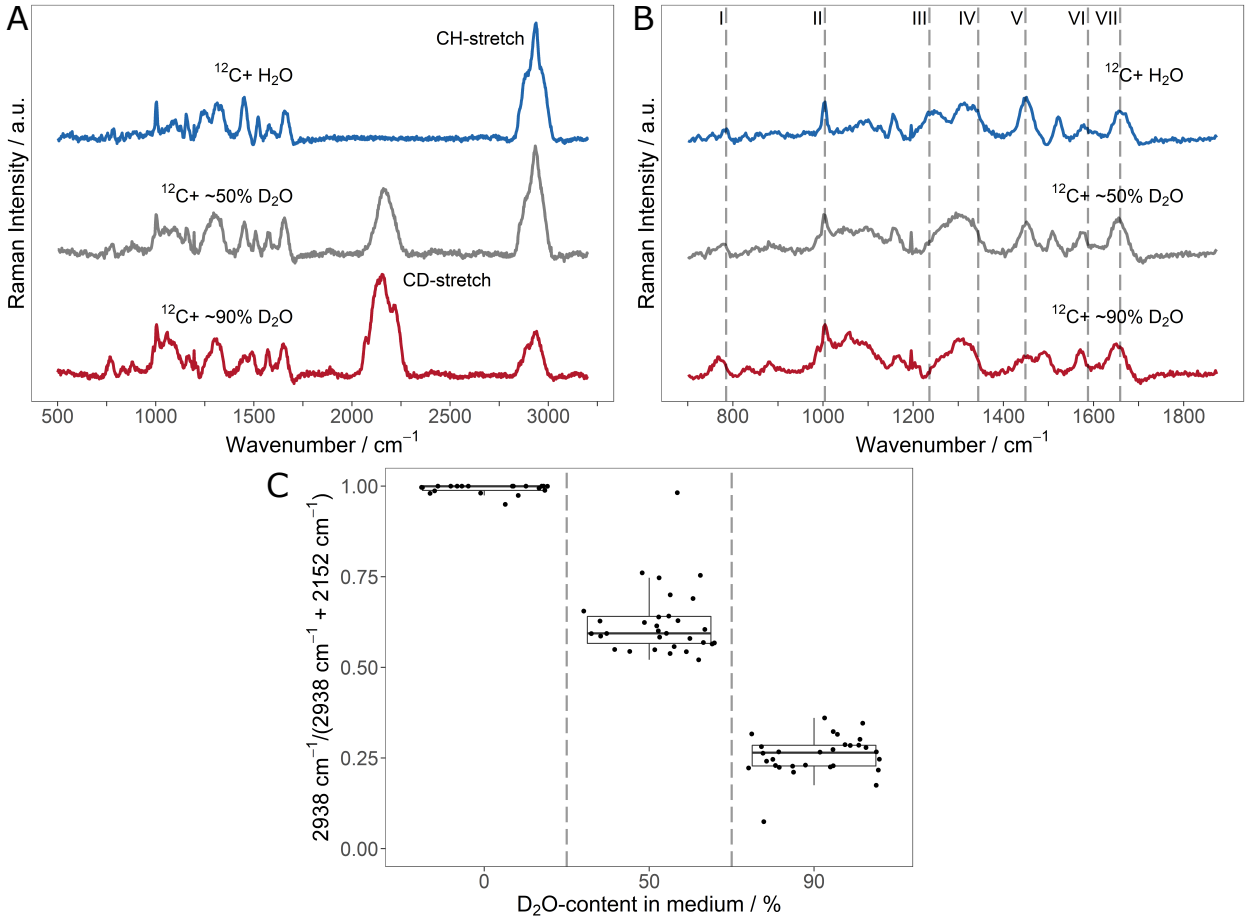

SI Figure 8: (A) Average single-cell Raman spectra (n = 20-30; 20 s integration time, 10 mW laser power) of *Sphingomonas sp.* grown in medium containing $^{12}C_6$-glucose and diverging ratios of H_2O/D_2O; (B) fingerprint area zoom of the spectra (700 cm^{-1} to 1800 cm^{-1}) with selected signals assigned to cellular biomolecules as follows:[12,13] I – $\nu(C,U,T)_{ring}$, II – $(Phe)_{ring\ breathing}$, III – $\nu(Amide\ III)$, IV – $\delta(CH_2)_{rocking}$, V – $\delta(CH_2)_{scissor}$, VI – $\nu(G,A)_{ring}$, VII – $\nu(Amide\ I)$ where U, C, T, G, A and Phe stand for uracil, cytosine, thymine, guanine, adenine and phenylalanine (ν = stretching mode, δ = bending mode); (C) ratio of the CH/CD-stretch signal integrals corresponding to unlabeled (CH-strech at 2938 cm^{-1}) and D-labeled (CD-stretch at 2152 cm^{-1}) cells for the individual spectra as a function of the D_2O-content in the medium.

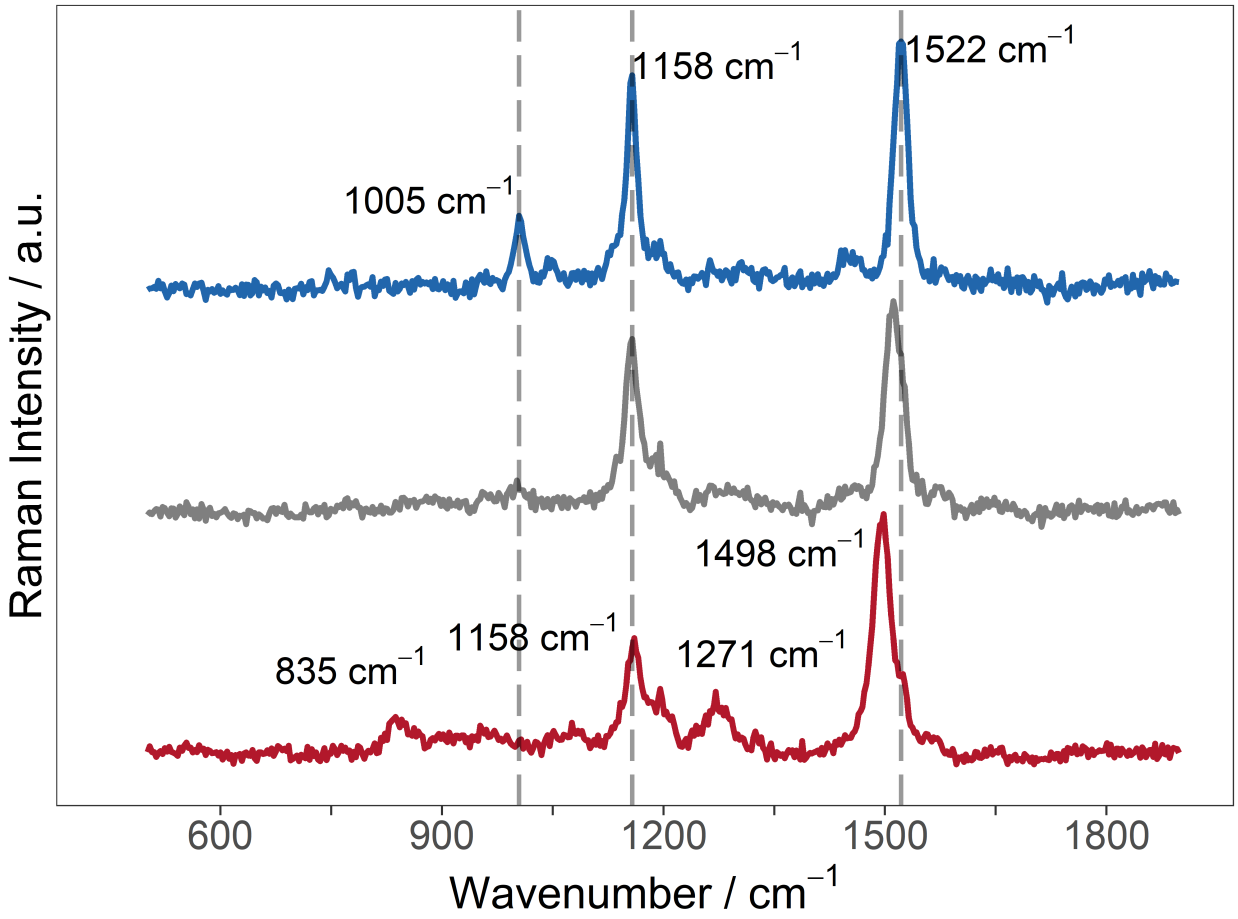

SI Figure 9: Average single-cell Resonance Raman spectra (n = 50, n = 25 for pure H_2O medium) as shown in Figure 3 A, but with broader range down to 500 cm^{-1} in order to highlight the absence of additional bands at lower wavenumbers; *Sphingomonas sp.* were grown in media containing $^{12}C_6$-glucose and diverging ratios of H_2O/D_2O; dashed lines correspond to the position of carotenoid signals of unlabeled bacteria.

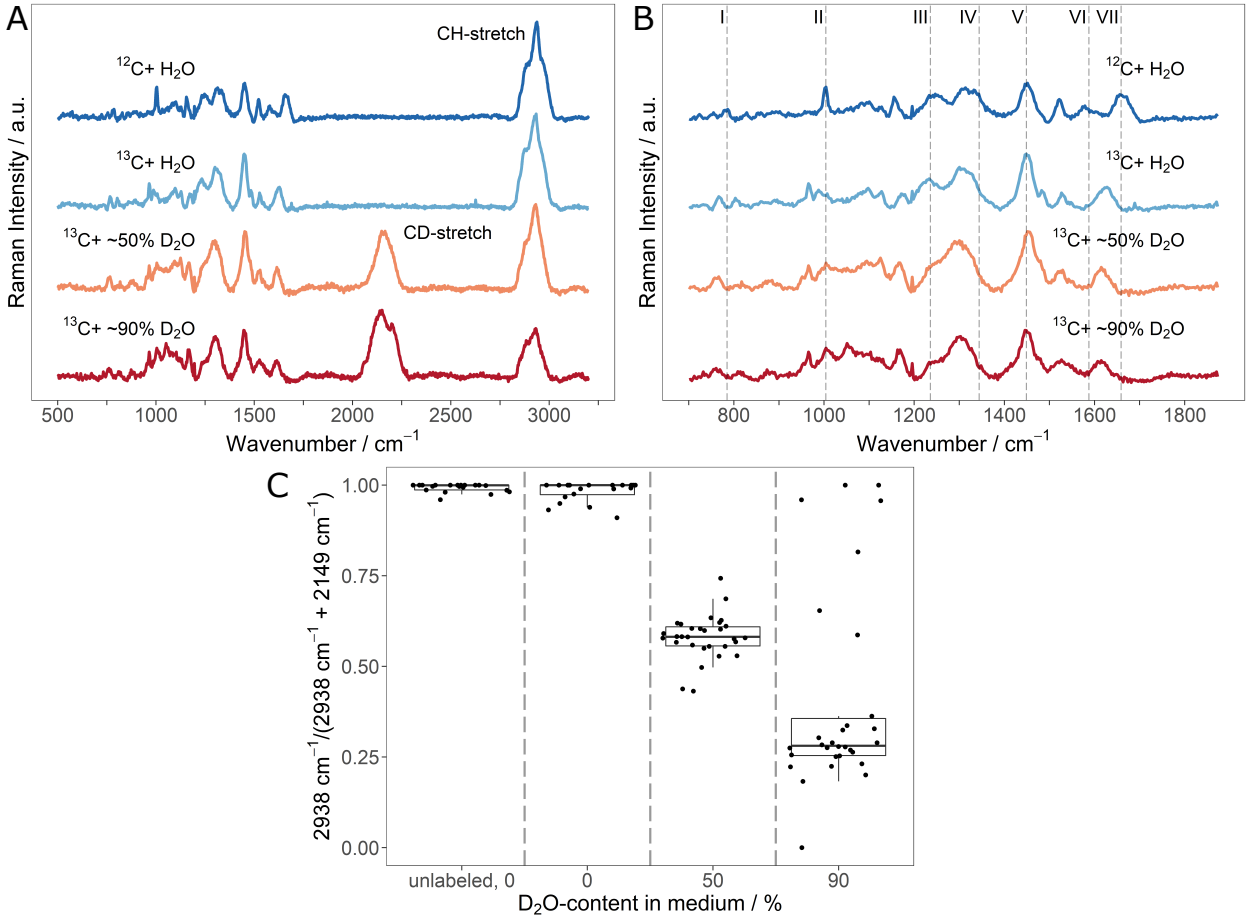

SI Figure 10: (A) Average single-cell Raman spectra (n = 20-30; 20 s integration time, 10 mW laser power) of *Sphingomonas sp.* grown in media containing $^{13}C_6$-glucose and diverging ratios of H_2O/D_2O (as a reference, the spectrum of unlabeled cells is shown in the top position); (B) fingerprint area zoom of the spectra (700 cm^{-1} to 1800 cm^{-1}) with selected signals assigned to cellular biomolecules as follows:[12,13] I – $\nu(C,U,T)_{ring}$, II – $(Phe)_{ring\ breathing}$, III – $\nu(Amide\ III)$, IV – $\delta(CH_2)_{rocking}$, V – $\delta(CH_2)_{scissor}$, VI – $\nu(G,A)_{ring}$, VII – $\nu(Amide\ I)$ where U, C, T, G, A and Phe stand for uracil, cytosine, thymine, guanine, adenine and phenylalanine (ν = stretching mode, δ = bending mode); (C) ratio of the CH/CD-stretch signal integrals corresponding to [^{1}H,^{13}C]-labeled (CH-strech at 2938 cm^{-1}) and [D,^{13}C]-labeled (CD-stretch at 2149 cm^{-1}) cells for the individual spectra as a function of the D_2O-content in the medium.

References

(1) Weiss, R.; Palatinszky, M.; Wagner, M.; Niessner, R.; Elsner, M.; Seidel, M.; Ivleva, N. P. Surface-enhanced Raman spectroscopy of microorganisms: limitations and applicability on the single-cell level. *The Analyst* **2019**, *144*, 943–953.

(2) Liland, K. H.; Almøy, T.; Mevik, B.-H. Optimal Choice of Baseline Correction for Multivariate Calibration of Spectra. *Applied Spectroscopy* **2010**, *64*, 1007–1016.

(3) Kuhn, M. caret: Classification and Regression Training. 2020; `https://CRAN.R-project.org/package=caret`.

(4) Locher, R. IDPmisc: 'Utilities of Institute of Data Analyses and Process Design (www.zhaw.ch/idp)'. 2020; `https://CRAN.R-project.org/package=IDPmisc`.

(5) Lê, S.; Josse, J.; Husson, F. FactoMineR: A Package for Multivariate Analysis. *Journal of Statistical Software* **2008**, *25*, 1–18.

(6) Wickham, H. *ggplot2: Elegant Graphics for Data Analysis*; Springer-Verlag New York, 2016.

(7) Müller, K.; Wickham, H. tibble: Simple Data Frames. 2020; `https://CRAN.R-project.org/package=tibble`.

(8) Dowle, M.; Srinivasan, A. data.table: Extension of data.frame. 2020; `https://CRAN.R-project.org/package=data.table`.

(9) developers, s. signal: Signal processing. 2014; `http://r-forge.r-project.org/projects/signal/`.

(10) Adler, D.; Murdoch, D., et al. rgl: 3D Visualization Using OpenGL. 2020; `https://CRAN.R-project.org/package=rgl`.

(11) Tschirner, N.; Schenderlein, M.; Brose, K.; Schlodder, E.; Mroginski, M. A.; Thomsen, C.; Hildebrandt, P. Resonance Raman spectra of beta-carotene in solution and in photosystems revisited: an experimental and theoretical study. *Physical chemistry chemical physics : PCCP* **2009**, *11*, 11471–11478.

(12) Huang, W. E.; Griffiths, R. I.; Thompson, I. P.; Bailey, M. J.; Whiteley, A. S. Raman microscopic analysis of single microbial cells. *Analytical chemistry* **2004**, *76*, 4452–4458.

(13) Ivleva, N. P.; Wagner, M.; Horn, H.; Niessner, R.; Haisch, C. Towards a nondestructive chemical characterization of biofilm matrix by Raman microscopy. *Analytical and bioanalytical chemistry* **2009**, *393*, 197–206.